Appl Biochem Biotechnol
DOI 10.1007/s12010-016-2048-1

The Use of Reverse Vaccinology and Molecular Modeling Associated with Cell Proliferation Stimulation Approach to Select Promiscuous Epitopes from *Schistosoma mansoni*

Flávio M. Oliveira[1] · **Ivan E. V. Coelho**[2] · **Marcelo D. Lopes**[1] · **Alex G. Taranto**[2] · **Moacyr C. Junior**[2] · **Luciana L. D. Santos**[1] · **José A. P. F. Villar**[1] · **Cristina T. Fonseca**[3] · **Débora D. O. Lopes**[1]

Received: 21 December 2015 / Accepted: 7 March 2016

Abstract Schistosomiasis remains an important parasitic disease that affects millions of individuals worldwide. Despite the availability of chemotherapy, the occurrence of constant reinfection demonstrates the need for additional forms of intervention and the development of a vaccine represents a relevant strategy to control this disease. With the advent of genomics and bioinformatics, new strategies to search for vaccine targets have been proposed, as the reverse vaccinology. In this work, computational analyses of *Schistosoma mansoni* membrane proteins were performed to predict epitopes with high affinity for different human leukocyte antigen (HLA)-DRB1. Ten epitopes were selected and along with murine major histocompatibility complex (MHC) class II molecule had their three-dimensional structures optimized. Epitope interactions were evaluated against murine MHC class II molecule through molecular docking, electrostatic potential, and molecular volume. The epitope Sm141290 and Sm050890 stood out in most of the molecular modeling analyses. Cellular proliferation assay was performed to evaluate the ability of these epitopes to bind to murine MHC II molecules and stimulate CD4+ T cells showing that the same epitopes were able to significantly stimulate cell

Electronic supplementary material The online version of this article (doi:10.1007/s12010-016-2048-1) contains supplementary material, which is available to authorized users.

✉ Débora D. O. Lopes
debora@ufsj.edu.br

[1] Laboratory of Molecular Biology, Universidade Federal de São João del Rei, Av. Sebastião Gonçalves Coelho, 400, Divinópolis, Minas Gerais 35501-296, Brazil

[2] Laboratory of Molecular Modeling, Universidade Federal de São João del Rei, Av. Sebastião Gonçalves Coelho, 400, Divinópolis, Minas Gerais 35501-296, Brazil

[3] Research Group in Parasite Biology and Immunology, Centro de Pesquisas René Rachou–Fundação Oswaldo Cruz, Av. Augusto de Lima, Belo Horizonte, MG 30190-002, Brazil

Published online: 16 March 2016

proliferation. This work showed an important strategy of peptide selection for epitope-based vaccine design, achieved by in silico analyses that can precede in vivo and in vitro experiments, avoiding excessive experimentation.

Keywords Schistosomiasis · Reverse vaccinology · Epitopes · Molecular docking · Cell proliferation

Introduction

Schistosomiasis is an important parasitic disease affecting over 230 million people worldwide and remains a significant cause of morbidity in 76 countries [1]. The disease is prevalent in tropical and subtropical areas, occurring in various regions of South America, Africa, and Asia [2]. Chemotherapy is one of the main strategies employed to treat schistosomiasis, yet constant reinfection, difficulties in mass treatment, poor sanitation, and reduced sensitivity of some parasite populations to praziquantel are factors which motivate the search for new strategies to control this disease [3, 4]. Development of a treatment strategy combining vaccine, chemotherapy, and socioeconomic interventions is a promising approach to achieve sustainable control of schistosomiasis [5].

Traditionally, vaccines have been developed by isolating and purifying antigenic components from a pathogen of interest, which is usually killed by heat or chemically inactivated. This model, however, does not apply to schistosomiasis, since irradiated cercariae presents a high risk of contamination during immunization [6]. Antigens tested in animals have shown promising potential for inducing protection as proteins Sm14, Sm28-GST, Sm97, TPI, IrV-5, Sm23, and Smp80. The Sm14 and Sm28-GST, used in vaccine formulations currently undergoing clinical trials, were capable to induce different levels of partial protection in animal models [7–9]. A vaccine against schistosomiasis that is not entirely sterilant, but which can significantly reduce the parasite worm is also a promising strategy, since it could be used along with chemotherapy [10].

The availability of new technologies and complete genomes of various parasites have contributed significantly to advances in the field of vaccinology. Among these technologies, bioinformatics has drawn considerable attention for its ability to predict biological processes, functions, and structures, orienting the subsequent experimental steps of research. Increasingly, bioinformatics software based on specific algorithms for gene and protein analysis are being developed and made available [11, 12]. In this context, reverse vaccinology emerged as a technique for determining the theoretical ability of molecules to induce immune responses, paving the way for the development of vaccines designed through in silico prediction of antigens [13–15]. Other important current tools in vaccine study is the structural vaccinology, an approach that came as a logical improvement of reverse vaccinology and it has shown important results in vaccine targets design and optimization [16, 17].

Schistosoma mansoni antigens are phagocytized and degraded in peptides (epitopes) by antigen-presenting cell (APC) of the host immune system to be presented to $CD4^+$ lymphocytes via major histocompatibility complex (MHC class II). MHC or human leukocyte antigens (HLAs) exhibit high diversity and specificity of interaction, though some epitopes, described as promiscuous, can be presented to $CD4^+$ lymphocytes by different HLAs, increasing the immune stimulation [18]. These interactions have an

important effect on immune response, especially in macrophages activation, B lymphocytes, and cytotoxic T cells [19]. Therefore, the investigation of interaction between MHC molecule and epitopes is essential to the rational development of vaccines against schistosomiasis and other diseases.

A number of methods are available for predicting peptide-binding to MHC molecules, including binding prediction based on peptide primary sequence and binding prediction based on three-dimensional structures, which provide improved understanding of the intermolecular interactions governing peptide recognition by MHC molecules [20]. Molecular docking has been used to predict the conformation of a small molecule (ligand) and a biomacromolecule (receptor), as well as the binding affinity between them. Docking methodology is able to rank a set of ligands based on their binding affinity and describe the main intermolecular interactions [21]. These data are useful for structure activity relationship (SAR) studies, directing for design of new activity compounds and vaccines. In our previous work, promiscuous epitopes were identified through bioinformatics tools and together with other epitopes of vaccine targets (Sm14, Sm29, Sm23, Sm10, and Sm21.7) were modeled with the N-terminal linked to a galactose moiety to improve immune response [13].

An approach combining in silico prediction of likely epitopes with experimental in vitro/in vivo validation of vaccine candidates has proved a highly valuable tool in vaccine search [22, 23]. In this study, ten epitopes predicted to have high affinity for main HLA-DRB1 were obtained from hypothetical protein database (HPD) constructed through bioinformatics analyses by our research group [13]. The epitopes were evaluated by theoretical assays using molecular mechanics calculation, docking simulation, electrostatic potential surface, and molecular volume to investigate interaction of these epitopes with murine MHC class II H2-IAb molecule. To validate in silico analyses, these epitopes were synthesized and used to immunize mice that were individually tested for their ability to stimulate $CD4^+$ T lymphocyte proliferation. Finally, the interactions of the epitopes that stood out in cell proliferation assay with HLA-DRB1 through molecular docking to predict the affinity with human immunological system were evaluated.

Materials and Methods

Ethics Statement

All protocols involving animals were approved by the Animal Care and Ethics Committee of the Federal University of São João del Rei (CEPEA–UFSJ 12/2010). The animals were maintained in the Laboratory Animal Facilities of the Federal University of São João del Rei in compliance with Brazilian Law 11749, issued in 2008, and Decree 6899, of 15 July 2009, which regulate animal care procedures and use of animals for scientific and educational purposes.

Epitope Selection

In our previous work, hypothetical proteins of as yet unrated immunogenic potential of *S. mansoni* were obtained from the GeneDB (http://www.genedb.org) and NCBI (http://www.ncbi.nlm.nih.gov/pubmed) databases (accessed in February 2012) and were analyzed through bioinformatics tools to predict cellular localization, peptide signal,

and topology [13]. The exposed regions of selected proteins were deposited in the hypothetical protein database (HPD).

Here, the proteins present in HPD were analyzed to predict epitopes with high affinity for HLA-DRB1 molecules using the software: NetMHCII 3.2 (http://www.cbs.dtu.dk/services/NetMHCII/), Rankpep (http://imed.med.ucm.es/Tools/rankpep.html), and Syfpeithi (http://www.syfpeithi.de/bin/MHCServer.dll/EpitopePrediction.htm). The biding affinities of all epitopes were evaluated for the HLA DRB1: 0101, 0301, 0401, 0701, 1101, and 1501 [24, 25]. Only epitopes of 15 amino acids with higher binding affinity scores for each HLA were selected. These predictors are constantly updated; for this reason, the HPD was recently reanalyzed.

The epitopes of each protein selected by the three software were aligned simultaneously for all HLAs with their respective exposed sequences using MultiAlin 5.4.1 software (http://multalin.toulouse.inra.fr/multalin). The epitopes that exhibited better overlap on alignment were selected for the subsequent analyses. Syfpeithi was also used to determine the number of HLA-DRB1 that bind to the selected epitopes.

Obtention of Three-Dimensional Structures of MHC II H2-IAb Molecule and Epitopes

The MHC II H2-IAb molecule was chosen to simulate the interaction with the selected epitopes. Crystallographic structure of MHC II H2-IAb, was obtained in the Protein Data Bank (PDB) (http://www.rcsb.org/pdb/home/home.do) under code 1MUJ and subjected to geometric optimization using the sander program of the Amber 11.0 package [26]. The structure was refined by energy minimization using the implicit solvent model developed by Hawkins, Cramer, and Truhlar [27, 28], with 10,000 cycles. The first 3000 cycles were calculated by the steepest descent method and the remainders by conjugate gradient with ff03 force field [29, 30], using a cutoff value of 14 Å for the interactions of unbound atoms. The epitopes selected by bioinformatics tools were generated in extended conformation using Gauss View 5.0 software [31] and subjected to the same geometric optimization process used for MHC class II H2-IAb molecule.

Molecular Docking Between Epitopes and MHC II H2-IAb

The refined structures were then subjected to molecular docking simulation using AutoDock Vina software [21]. Docking simulations were performed keeping the main chain rigid in extended conformation, whereas the side chains were left flexible. A sufficiently large grid box was generated (60 Å × 36 Å × 28 Å, with 1-Å spacing between grid points) covering the entire binding site. The method was validated by redocking using H2-IAb molecule with its respective ligand [32]. Finally, docking was performed to predict the bound conformations and the interactions of the selected epitopes with MHC II H2-IAb molecule.

Calculating the Electrostatic Potential Surface and Molecular Volume

After molecular docking, electrostatic potentials were calculated for H2-IAb molecule and for all the epitopes and CLIP (peptide complexed with H2-IAb molecule obtained in the PDB) using AutoDock Tools software [33]. An electrostatic potential surface was generated to verify whether the binding region of the MHC II molecule exhibited electrostatic complementarities

to epitope potential surfaces. Furthermore, the molecular volume of the epitopes and CLIP using Discovery Studio 4.1 was verified [34].

Synthesis of Selected Epitopes

The epitopes were synthesized by solid-phase chemistry and purified for high-performance liquid chromatography definition by Rheabiotech Ltd. (Brazil). The epitopes were diluted in 5 % dimethyl sulfoxide (DMSO) and phosphate-buffered saline (PBS) (0.14 M NaCl, 0.02 M KCl, 0.01 M KH_2PO_4, 0.08 M Na_2HPO_4) at a concentration of 100 μg/μL and stored at −20 °C.

Proliferation Assays

Female C57BL/6 mice aged 6–8 weeks, acquired from the Unicamp Central Animal Facilities (Campinas, Brazil), were treated with antiparasitic drugs 10 days before the experiments, as described elsewhere [35]. A group of ten animals were immunized with three subcutaneous doses (15 days apart) of a mixture containing 10 μg of each epitope diluted in 100 μL of PBS. The vaccine was formulated with complete Freund's adjuvant (Sigma) in the first immunization and incomplete Freund's adjuvant (Sigma) in subsequent immunizations.

One week after the last immunization, the animals were euthanized, and spleen cells were obtained to evaluate $CD4^+$ T lymphocyte proliferation in response to in vitro restimulation with each epitope individually [36]. To this end, the spleens of the immunized mice were excised and macerated, and their red cells lysed with lysis buffer (0.15 M NH_4Cl, 1 M $KHCO_3$, 0.1 M Na_2EDTA). After several washes with sterile saline solution and centrifugation, the lysed red cells were separated from the splenocytes and the latter were resuspended in complete Roswell Park Memorial Institute (RPMI) medium (Gibco) containing 10 % complete fetal bovine serum (Gibco) and 1 % penicillin–streptomycin (Gibco). The cells were adjusted to a concentration of 10^7 cells per milliliter and 7.5 μM of the carboxyfluorescein fluorochrome succinimidyl ester (CFSE) (Sigma) was added to the volume. The tubes were then centrifuged and the cells adjusted to 5×10^5 labeled cells per well using complete RPMI. The experiment was performed in duplicate.

Ten micrograms of each epitope were individually added to the culture wells to stimulate cell proliferation. As control assay, the CFSE-labeled splenocytes were maintained in complete RPMI medium or concanavalin A (ConA) at a final concentration of 5 μg/mL. The plates were incubated in a 5 % CO_2 atm at 37 °C for 72 or 120 h. After incubation, CFSE-labeled spleen cells were labeled with anti-mouse CD4 biotin antibody for investigation of $CD4^+$ proliferation. The spleen cell cultures were centrifuged, the supernatant discarded, and the cells incubated with 0.175 μg of anti-CD16/CD32 antibodies (e-bioscience) to block the Fc receptor. The cells were then incubated with 0.25 μg of biotinylated anti-mouse CD4 antibodies (BD-Bioscience) and subsequently bound to streptavidin conjugated to the fluorochrome allophycocyanin (APC) (1:200). Each type of antibody and the streptavidin conjugate were diluted in PBS, 0.5 % bovine serum albumin (BSA), and 2 mM sodium azide before being added to the wells. After washing to remove unbound antibodies, the cells were finally fixed with 2 % formaldehyde diluted in PBS and stored at 4 °C.

Cell data were collected using an LSR-Fortessa cytometer and analyzed with FlowJo7.6.5 software (Tree Star, OR, USA) [37].

Statistical Analysis

Statistical analysis was performed using GraphPad Prism 5.0 software (San Diego, CA, USA). The data obtained in the proliferation assay were analyzed using analysis of variance (ANOVA), followed by Dunnett's test for multiple comparison.

Molecular Docking Between Selected Epitopes and HLA-DRB1 Molecule and Calculating of the Electrostatic Potential

Electrostatic potential and intermolecular interactions between the epitopes that stood out in the proliferation assay and HLA-DRB1 molecules (0101, 0301, 0401, and 1501) were determined through of the same methodology used for MHC II H2-IAb molecule. The HLA-DRB1-0701 and HLA-DRB1-1101 molecules were not analyzed since their structures are not available in the Protein Data Bank (PDB). The crystallographic structures of the HLA-DRB1 0101 molecule, HLA-DRB1 0301, HLA-DRB1 0401, and HLA-DRB1 1501 are deposited in the PDB under codes, 1DLH, 1A6A, 2SEB, and 1BX2, respectively.

Results

Prediction, Alignment, and Selection of Epitopes

A total of 25 exposed regions deposited in the HPD, identified in our previous work [13], were analyzed for affinity prediction of epitopes for different HLA-DRB1. In total, about 500 different 15 amino-acid epitopes were predicted that exhibited highest scores of affinity for HLA-DRB1 considered. Through alignment of all epitopes obtained with exposed regions present in the HPD, ten promiscuous epitopes were selected, corresponding to the ones most strongly recognized by all HLA-DRB1 molecules analyzed. Figure 1 exemplifies the alignment of the exposed region of Sm050890 with predicted epitopes. Of the ten selected epitopes, four coincide with our previous work [13] and the other ones stood out in this recent analysis (Table 1).

Syfpeithi program was also employed to reveal the number of HLA-DRB1 capable of binding to selected epitopes from the target proteins. Each column in Fig. 2 represent the number of HLA-DRB1 with high affinity at the least part of the selected epitopes. Seven out of ten epitopes showed high affinity for at least five HLA-DRB1.

Three-Dimensional Structures of MHC II H2-IAb and Epitopes

The MHC II H2-IAb structure was obtained from the PDB (code 1MUJ) complexed with its corresponding ligand (CLIP). As the peptides only interact with MHC molecules in extended conformation, their three-dimensional structures were constructed and optimized using this conformation. This procedure of minimizing structure energy ensures that any features leading to an energetically unstable structure (atom contact, bond distances, bond angles, or dihedral conformation) are eliminated (data not shown).

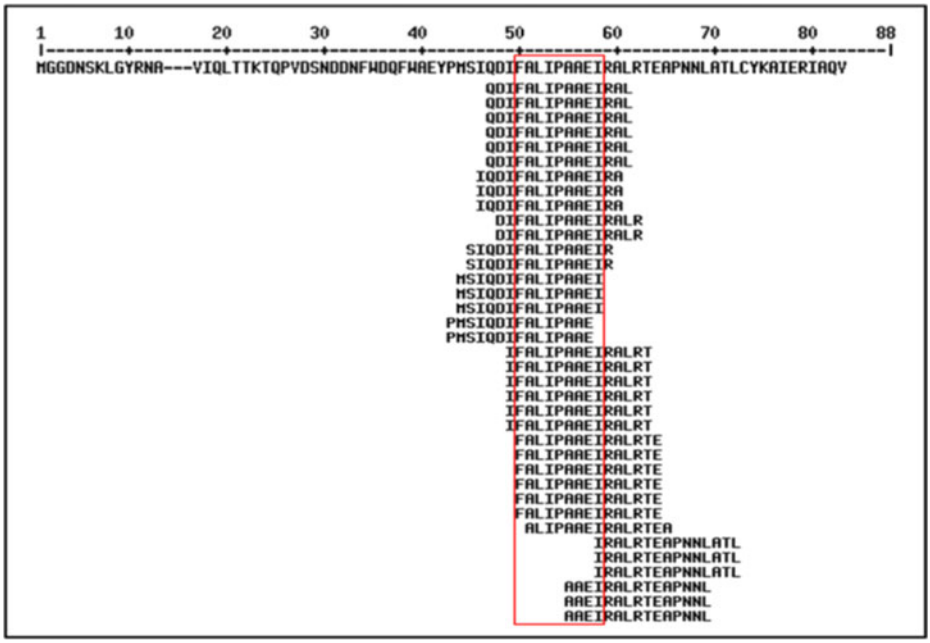

Fig. 1 Alignment between epitopes predicted for different HLA-DRB1 and protein Sm050890. The *highlighted area* shows the alignment of a sequence common to all three epitope prediction programs for all HLA-DRB1 analyzed. Alignments were performed using MultiAlin 5.4.1 software

Molecular Docking Between MHC II H2-IAb and Epitopes

The optimized three-dimensional structure of MHC II H2-IAb molecule and the peptide obtained from the PDB was employed for peptide redocking to validate the molecular docking simulation. Low value of root-mean-square deviation (RMSD) of 1.58 Å was obtained for heavy atoms of peptide fitted into H2-IAb molecule. A RMSD threshold of 2 Å is often adopted to indicate suitable prediction of binding conformation [21]. As shown in Fig. 3, good overlapping occurred in the conformation of the ligand subjected to molecular redocking,

Table 1 Epitopes selected by reverse vaccinology

GeneDB	NCBI	Epitope sequence	Position
Sm135880	CCD82381.1	TFYFPRSTTIHLKQS	80 to 94
Sm149930.1	CCD79088.1	VFSRFLQILQTPIFL	583 to 597
Sm149930.2	CCD79088.1	KHVMVHANSRPFICC	105 to 119
Sm145420	CCD79353.1	AFRYRSLPNNLNFQD	285 to 299
Sm144970	XP_002575547.1	IQVFDSTRATSLGSV	88 to 102
Sm141880	XP_002575023.1	IQFYLTSDCLLNSEM	267 to 281
Sm050890	XP_002576389.1	QDIFALIPAAEIRAL	44 to 58
Sm141730	XP_002574997.1	SGWLYLAQPLITYSS	52 to 66
Sm145460	XP_002575652.1	QYQPQAAKTLLVRSA	177 to 191
Sm141290	XP_002582151.1	GFGLTVANHIRAGRD	225 to 239

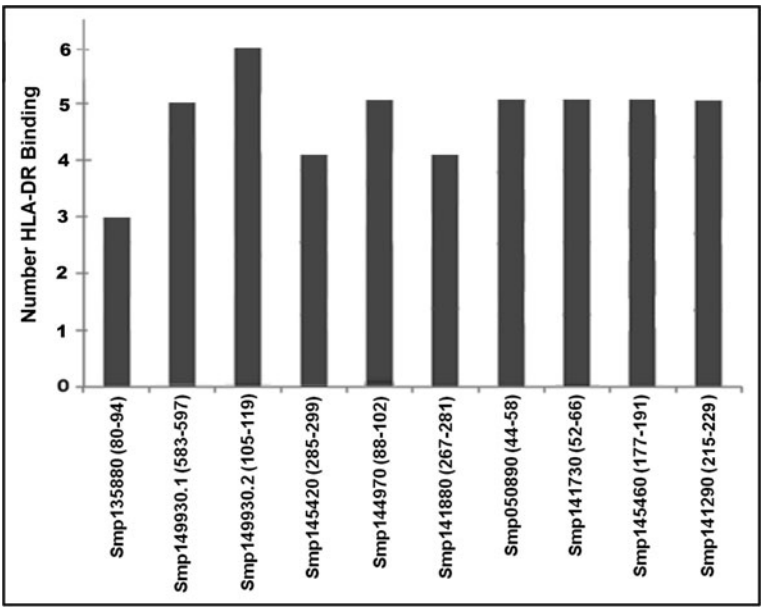

Fig. 2 Evaluation of number of HLA-DRB1 that binds to selected epitopes. Each *column* represents the number of HLA-DRB1 (0101, DRB1 0301, DRB1 0401, DRB1 0701, DRB1 1101, and DRB1 1501) with high affinity least part of the selected epitopes, according to Syfpeithi software

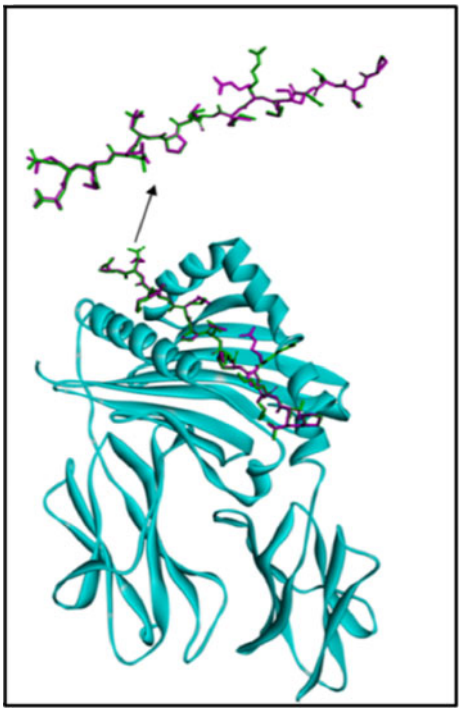

Fig. 3 Simulation of redocking between MHC II H2-IAb molecule and its respective ligand. Conformation of ligand after molecule redocking (*pink*) superimposed to the respective crystallographic structure optimized by Amber 11.0 (*green*) for and H2-IAb

compared with the optimized structure, demonstrating the suitability of the method for determining interaction between epitopes and MHC II H2-IAb molecule.

After redocking, molecular docking was performed for all epitopes and MHC II H2-IAb molecule. The Table 2 shows the total number of interactions (hydrogen bond/electrostatic interactions/van der Waals/π interactions) of each epitope and of the CLIP ligand with MCHII H2-IAb binding site.

Electrostatic Potential Surface of the MHC II H2-IAb and Epitopes

The higher complementarity between electrostatic potential surfaces (EPS) of the ligand and receptor the better will be its interaction. The EPS is calculated through a grid posed on the structure of the ligand and receptor and is based on the atomic charges. The choice of the way of charge calculation is critical to the accuracy of the results. In the model used, the atomic charges were calculated by Gasteiger method [38, 39].

Figure 4 shows the EPS of the MHC II (A) and the CLIP (B). Del Carpio and co-workers showed importance of this complementarity to the interaction between epitopes and MHC I and this must be true to the interaction between epitopes and MHC II as well [40]. The receptor contains two regions of opposite polarities and some cavities where key residues, whose right polarity would enable binding to occur. Figure 4b depicts the electrostatic potential surfaces of the CLIP. The right end shows a positive potential (the blue portion), which interacts with the red portion of the MHC II H2-IAb molecule with negative potential. The other end of the epitope has negative polarity, thereby interacting with the positive potential of the receptor.

Table 3 shows the upper and lower limits of the values of electrostatic potential and molecular volume for each epitope and the CLIP. In addition, the electrostatic map (supplementary file) shows the possible interaction regions due to electrostatic complementarity. These values appear to be important once the molecules require not only correct orientation, but also values of the interacting portions of the complex that allow stable binding to take place. The results show that epitopes Sm050890 and Sm141290 have values and polarity distribution similar to those exhibited by the CLIP molecule, thus revealing a high potential for interaction with the MHC II H2-IAb molecule. The CLIP and the epitopes Sm144970,

Table 2 Number of intermolecular interactions between epitopes and H2-IAb molecule

	Hydrogen bound	Electrostatic interactions	van der Waals	π interactions	Total
Sm144970	5	6	10	0	21
Sm141880	6	9	7	1	23
Sm141730	4	7	13	0	24
Sm050890	4	6	15	0	25
Sm135880	0	8	18	0	26
Sm145460	4	9	14	1	28
Sm149930.1	6	7	16	0	29
Sm149930.2	9	10	13	0	32
Sm145420	8	12	15	0	35
Sm141290	8	12	13	2	35
CLIP	16	10	21	0	47

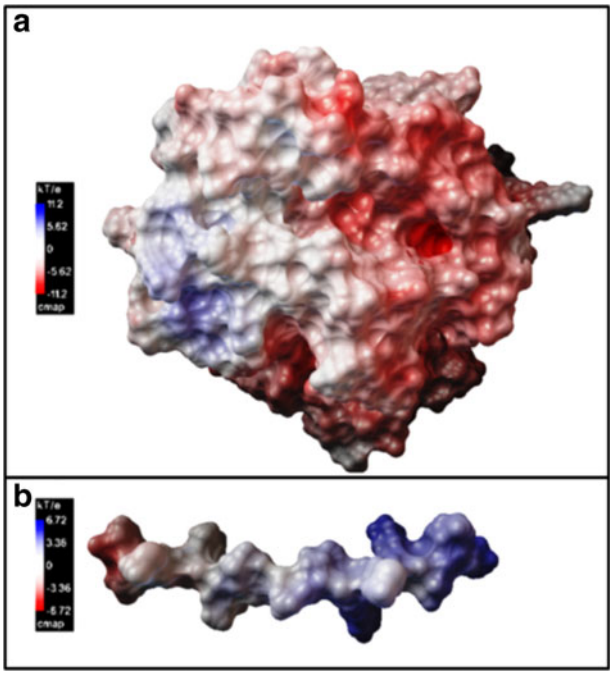

Fig. 4 Electrostatic potential map of MHC II H2-IAb molecule and CLIP ligand. Electrostatic complementarity between ligand (**b**) and MHC protein (**a**) where regions of positive potential (*blue*) interact with regions of negative potential (*red*)

Sm050890, Sm141730, Sm145460 and Sm141290 shows lower molecular volume (Table 3), which can favor the interaction with MHC II H2-IAb molecule.

Epitopes Estimulate CD4$^+$ T Lymphocytes Proliferation

Leukocytes obtained from the spleen of mice immunized with a mixture of ten epitopes were isolated and through by flow cytometry separated into areas according to physical feature size (FSC) versus granularity (SSC) for selection of lymphocyte populations of interest.

Table 3 Electrostatic potential and van der Waals volume (Å^3) of epitopes and CLIP ligand

	KT/e	Volume
CLIP (Ligand)	±6.72	1592.54
Sm135880	±5.64	1716.11
Sm149930.1	±5.89	1754.00
Sm149930.2	±10.6	1611.16
Sm145420	±9.71	1722.30
Sm144970	±6.17	1475.95
Sm141880	±8.24	1622.72
Sm050890	±6.23	1563.59
Sm141730	±4.69	1571.30
Sm145460	±5.46	1585.33
Sm141290	±6.39	1458.01

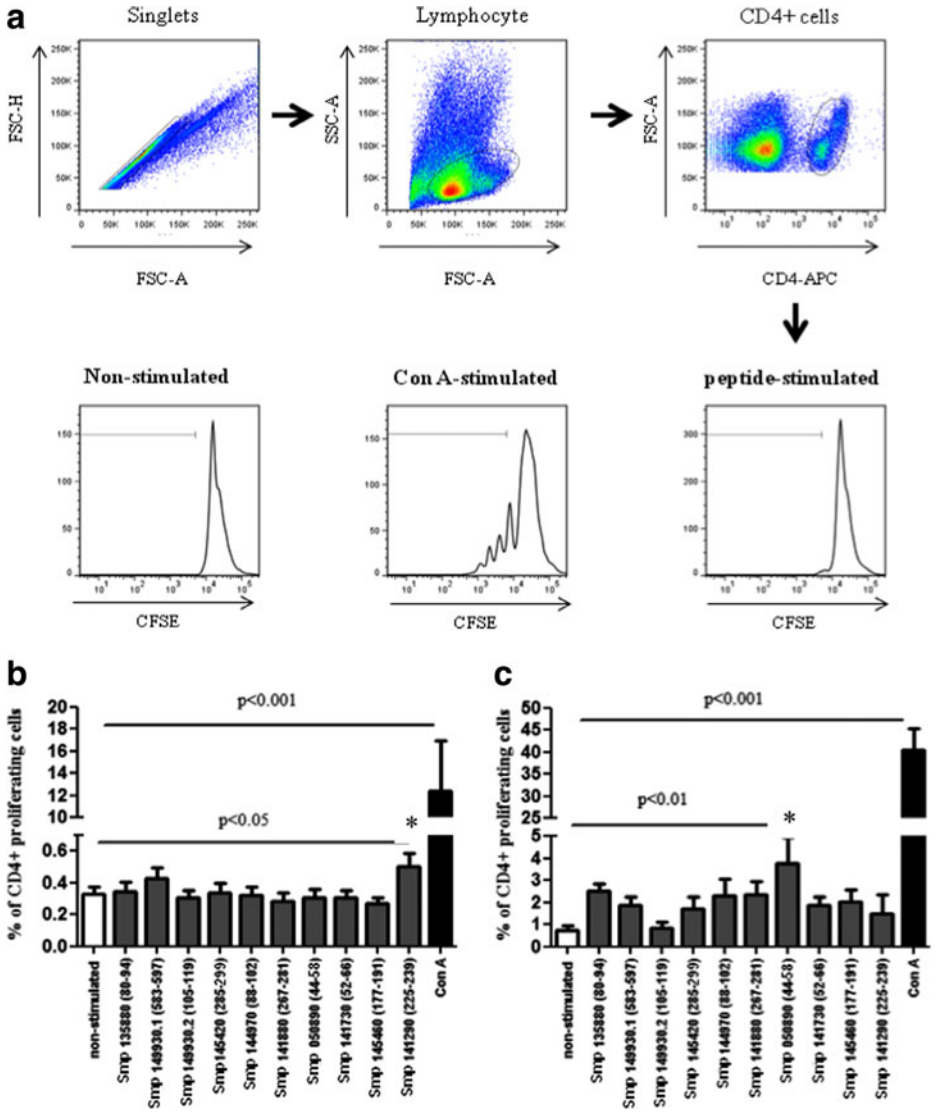

Fig. 5 Assessment of epitope-stimulated $CD4^+$ T lymphocyte proliferation. **a** $CD4^+$ T lymphocyte population selected according to the decrease of CFSE after each cell division cycle; **b** 72-h cell culture; and **c** 120-h cell culture. Statistically significant differences in proliferation ($p < 0.05$) between peptide groups and negative control (medium) and between positive control (ConA) and negative control are indicated in the graph (*asterisk*)

Subsequently, $CD4^+$ T lymphocytes were selected and proliferation levels were recorded, based on the decreasing content of CFSE in $CD4^+$ T lymphocytes after each cell division cycle (Fig. 5a).

The proliferation levels of labeled $CD4^+$ T lymphocytes stimulated with each of the ten epitopes were expressed as percent cell proliferation rates using FlowJo 7.6.5 software and compared with the non-stimulated cells. Statistical analysis (ANOVA followed by Dunnett's) revealed significant proliferation upon stimulation by epitope Sm141290 in 72-h cultures and Sm050890 in 120-h cultures (Fig. 5b, c).

Interactions Between Sm050890 and Sm141290 Epitopes and HLA-DRB1

Molecular docking of the Sm050890 and Sm141290 epitopes with HLA-DRB1 molecules was performed to determine the number of interactions and the limits of the values (upper and lower) of electrostatic potential. The total number of intermolecular interactions (hydrogen bond/electrostatic interactions/van der Waals/π interactions) and the electrostatic potential values for each epitopes and the ligand (peptide complexed with HLA-DRB1 molecules obtained in the PDB) with different HLAs are shown in Tables 4 and 5, respectively.

Discussion

No fully effective vaccine against schistosomiasis has been developed as yet. Therefore, a vaccine capable of significantly reducing worm burden represents a promising strategy, as it could be used in conjunction with chemotherapy [10]. Advances in bioinformatics and molecular biology have been providing the development of innovative strategies such as reverse vaccinology that predict potential immunity-inducing peptides using computational analyses [41, 42].

In our previous work, we have identified some vaccine targets using bioinformatics tools. Twenty-five hypothetical membrane proteins were selected and their exposed regions identified to predict the promiscuous epitopes. Nine of them were modeled with the N-terminal linked to a galactose moiety, to form glycoconjugate structures, and had their structural stability evaluated through molecular dynamics simulations. The sugar addition in these molecules was adopted to improve the immune response in biological assays [13].

Now, using the same database (HPD) composed by 25 proteins, we proposed the use of refined computational analyses allied to in vitro assay, in vaccine target screening. Theoretical in silico studies such as the present investigation involved reverse vaccinology and methods based on molecular mechanics, including molecular docking simulation, determination of electrostatic potential, and molecular volume. These techniques can estimate the interactions among vaccine targets and immune system and their ability to induce immune response in animals can be evaluated after this selection, reducing the need of excessive experimentation [17, 43]. Based on the available body of evidence, ten proteins were selected from sequences deposited in HPD, and were recently analyzed for prediction of epitopes with high affinity for HLA-DRB1. Among them, four epitopes coincided with those described previously by our research group [13] and other six epitopes stood out in this new screening. The different results observed between our works are due to frequent update of the predictors programs used. As observed in Fig. 2, seven epitopes showed high affinity for at least five HLA-DRB1, being considered promiscuous epitopes.

Table 4 Number of intermolecular interactions for epitopes Sm050890, Sm141290, and the ligand with different HLAs

HLADRB1				
	0101	0301	0401	1501
Sm050890	21	23	18	26
Sm141290	24	30	25	30
Ligand	44	39	49	38

Table 5 Electrostatic potential values for epitopes Sm050890, Sm144290, and the ligand with different HLAs

KT/e

	HLADRB1-0101	HLADRB1-0301	HLADRB1-0401	HLADRB1-1501
Sm050890	±6.13	±6.26	±6.14	±6.29
Sm141290	±6.43	±6.2	±6.55	±6.22
Ligand	±7.15	±6.76	±7.2	±6.13

In our previous work, the epitope Sm149930.1 was predicted as present in an exposed region of protein, and in our recent analyses, it was predicted as epitope of inner region. In the recent analyses, this epitope again highlighted in affinity prediction to HLA-DRB1; then, we decided to maintain this epitope in our study. We believe that this protein can reveal some important information in our future biological assays. Our goal is use the inner part of this protein as control in immune protection assay because this region is not accessible to immune system during parasite meeting, acting as a control of our in silico vaccine selection [24].

The most proteins previously described as hypothetical have now a functional statement provided; the functions were predicted through sequence similarity search [44]. One of our vaccine targets selected, Sm050890, maintained the status hypothetical protein and the other, Sm141290, as predicted as an innexin, a member of a family of proteins that create gap junctions in invertebrates. The innexin proteins have four transmembrane spanning units and the vertebrate connexin gap junction protein [45].

The ten epitopes had their affinity for MHC II- H2-IAb molecule estimated. Docking simulation showed the intermolecular interactions (Table 2) and ligand pose on binding site of MHC II H2-IAb molecule. The intermolecular interactions and steric effects are the driven forces to molecular recognition [32]. In this context, the epitopes Sm141880 and Sm144970, with a fewer number of intermolecular interactions and bulk residues, cannot fit properly in the binding site, resulting in a decrease of the affinity. Thus, new simulation can be performed to optimize the design of new activity peptides that can achieve the whole the biding site. The most active epitope Sm141290 can bind to active site through hydrogen bonds (HB), van der Waals (vW), electrostatic interaction (EI), and π interactions (PI) as well. As can be observed in Table 2, the total number of intermolecular interactions of epitope Sm141290 is bigger than epitopes Sm141880 and Sm144970. The difference is significantly, the epitope Sm141290 had 2 HB, 6 vW, 3 EI, and 1 PI more than epitope Sm141880 and 3 HB, 3 vW, 6 EI, and 2 PI more than epitope Sm144970. These finding explain the best profile of affinity of epitope Sm141290 for MHC II H2-IAb. Consequently, its increased number of interaction with this molecule contributes for the biological activity [46]. Furthermore, these results suggest that the designed peptides should be following this standard in the respective position for the molecular recognition. In addition, the most active epitopes in proliferation assay (Sm141290 and Sm050890) had the low and similar molecular volume to CLIP (Table 3). The H2-IAb molecule has a relatively narrower peptide-binding groove and epitopes with several bulky side chain may cause unfavorable interactions [47].

The electrostatic potential maps (supplementary file) can give a clue about the interactions between MHC II H2-IAb molecule and selected epitopes. The electrostatic potential is

calculated taking into account the distribution of charges along regions expected to interact with each other. Gilson and co-workers demonstrated the equivalence of calculated and experimental electrostatic potential values of particular amino acids [48], whereas Weiner [49] showed how electrostatic potential could be employed to elucidate the complementarity of receptor–ligand interactions. Electrostatic potential depends on the distribution of electric charges in the chemical structure and can be calculated in different manners [50, 51] by altering the conformation of the electrostatic surface potential, yet its principal features are retained by all the methods employed [52]. An important point in in silico study is the evaluation of interaction between epitopes and its binding region on the MHC molecule. This must exhibit electrostatic complementarity between the potential surfaces of ligand and receptor, as seen in the electrostatic potential map of H2-IAb and human CLIP (PDB code 1MUJ) (Fig. 4). The H2-IAb molecule clearly exhibits two regions of opposite polarities. Figure 4b shows the portion contacting the ligand-binding regions of the MHC molecule. The blue portion, of positive potential, strongly interacts with the red portion of the H2-IAb molecule, the cavity which has strong negative potential. The other end of the epitope, however, has negative polarity, thereby interacting with the positive potential of the H2-IAb molecule.

The distribution seen in the electrostatic potential (Table 3) is clearly similar between the epitope Sm141290 with the found for the PDB-retrieved CLIP. Furthermore, two relatively bulky residues (Ala and Thr) of Sm141290, docked into the more electronegative cavities of the receptor, whereas a more electronegative potential can be seen in the region interacting with the receptor in the electropositive region (supplementary file). The values of the electrostatic potential surface of epitope Sm141290 lay between ±15.84 kJ/mol or ±6.39 kT/e, while the value for CLIP is ±16.66 kJ/mol or ±6.72 kT/e. The second best in electrostatic potential surface analysis was obtained with epitope Sm050890, which has in its molecule the necessary portions to correctly interact with the pockets in the MHC II molecule (supplementary file). Moreover, the electrostatic potentials were in the range of ±15.44 kJ/mol or ±6,23 kT/e. The experimental data revealed that both epitope could form a stable interaction with the murine MHC II molecule. Other factors must therefore be at work, so as to explain the results and the value of the electrostatic potential and possibly operate in conjunction with a suitable distribution of polarities.

In order to draw a valid comparison, the potential regions of epitope Sm145460 were found to elicit the poorest stimulatory response in the experimental test and not to be complementary to the binding region on the MHC II H2-IAb molecule (supplementary file). Three factors appear to contribute to the low response observed. First, the distribution of positive potential almost completely covers the portion shown, yet a small region of negative potential appears beyond the Gln residue. Secondly, the residue distribution does not favor the interaction in spatial terms, due to the bulky region at the right end of the epitope (residues Gln, Tyr, and Gln) preventing it from sufficiently approaching interaction cavities, precluding effective docking. Finally, the electrostatic potential values (±5.89 kT/e or ±13.53 kJ/mol) were lower than those found for epitopes Sm050890 and Sm141290.

Table 3 depicts the electrostatic potential surface for epitopes Sm135880, Sm149930.1, and Sm141730, whose energy involved in the interaction between epitopes and MHC II H2-IAb molecule is lower than that observed for CLIP and epitopes Sm050890 and Sm141290. The inverse pattern of potential observed for epitopes Sm149930.2, Sm145420, and Sm141880, can be clearly noted, suggesting that these

energy values may be important to explain the poor results experimentally obtained with these epitopes.

The results of the proliferation assay showed that the epitopes Sm050890 and Sm141290 were able to stimulate significant $CD4^+$ T proliferation murine. For this reason, both epitopes were docked with HLA-DRB1 to evaluate the possible interactions. Table 4 shows the number of interaction of the Sm050890 and Sm141290 epitopes and ligand with HLA-DRB1. In addition, as observed in Table 5, both epitopes showed electrostatic potential values similar to ligand, mainly by HLA-DRB1 0301 and 1501, suggesting that the interaction between the epitopes and these HLAs can be more favorable. These analyses reveal that these epitopes establish several interactions with HLA-DRB1, suggesting that both can be presented in stimulation of immune system in possible human trials. As noted by Engelhard, the large variation in size and shape in epitopes that bind to MHC II structures can lead to interactions of scant biological relevance. For this reason, observations based on electrostatic potential data can suggest useful features for accurately describing the interaction taking place between epitope and MHC II molecule and for clarifying differences in immune responses [53].

The goal of the cellular proliferation assay performed in this study was assessing the ability of selected epitopes to stimulate $CD4^+$ T cell proliferation, to compare with in silico and modeling results and validate the strategy here proposed. It was observed that the Sm141290 and Sm050890 epitopes stood out in most computational analyses and were capable to significantly stimulate cell proliferation (Fig. 5). However, the analysis of intermolecular interactions does not favor the Sm050890 epitope. Nevertheless, this epitope was capable of stimulating cell proliferation, suggesting that electrostatic potential and molecular volume were more efficient in interaction for this epitope with MHC murine.

Zhao and co-workers observed significant proliferation of $CD4^+$ T lymphocytes stimulated for promiscuous epitopes of proteins from *S. japonicum* selected by reverse vaccinology, strengthening the use of this strategy in the search for immunogenic epitopes [54].

Flow cytometry analysis demonstrated that epitope Sm141290 significantly stimulated $CD4^+$ T lymphocyte proliferation, in comparison with the negative control (RPMI medium) in 72-h cell cultures (Fig. 5b), as did epitope Sm050890, albeit only in 120-h cultures (Fig. 5c). As the cells stimulated in the immunization were restimulated in vitro with each epitope separately, it was possible to detect specific $CD4^+$ T cell proliferation and thus use a negative control in this assay alone. These results show that epitope Sm141290 had higher stimulation capacity than epitope Sm050890 within the first few hours of cellular stimulation. With time, however, the ability of epitope Sm141290 stabilized, while that of epitope Sm050890 increased significantly, suggesting that both epitopes have highest potential to stimulate proliferation of $CD4^+$ T lymphocytes among all the epitopes tested [55]. Together, the results presented here emphasize the importance of in silico predictions in vaccine target screening before moving forward to vaccination trials, saving financial resource and animals.

Conclusion

The results obtained revealed a novel selection strategy of vaccine targets against schistosomiasis using reverse vaccinology to predict epitopes with high affinity for main HLA-DRB1, evaluation of MHCII H2-IAb affinity to selected epitopes through molecular modeling and validation of in silico analysis using cell proliferation stimulation assay.

References

1. WHO (2010). Schistosomiasis. Fact sheet no 115. WHO Media centre: World Health Organization.
2. Secor, W. E. (2014). Water-based interventions for schistosomiasis control. *Pathogens and Global Health, 108*(5), 246–254.
3. King, C. H., Olbrych, S. K., Soon, M., Singer, M. E., Carter, J., & Colley, D. G. (2011). Utility of repeated praziquantel dosing in the treatment of schistosomiasis in high-risk communities in Africa: a systematic review. *PLoS Neglected Tropical Diseases, 5*, 1–15.
4. Sabra, A. N., & Botros, S. S. (2008). Response of *Schistosoma mansoni* isolates having different drug sensitivity to praziquantel over several life cycle passages with and without therapeutic pressure. *Journal of Parasitology, 94*, 537–541.
5. Oliveira, S. C., Fonseca, C. T., Cardoso, F. C., Farias, L. P., & Leite, L. C. (2008). Recent advances in vaccine research against schistosomiasis in Brazil. *Acta Tropica, 108*, 256–262.
6. Souza, C. P., Araújo, N., Jannotti, L. K., & Gazzinelli, G. (1987). Factors that might affect the creation and maintenance of infected snails and the production of *Schistosoma mansoni* cercariae. *Memórias do Instituto Oswaldo Cruz, 82*, 73–79.
7. McManus, D. P., & Loukas, A. (2008). Current status of vaccines for schistosomiasis. *Clinical Microbiology Reviews, 21*(1), 225–242.
8. Bethony, J. M., Cole, R. N., Guo, X., Kamhawi, S., Lightowlers, M. W., Loukas, A., et al. (2011). Vaccines to combat the neglected tropical diseases. *Immunological Reviews, 239*(1), 237–270.
9. Fonseca, C. T., Oliveira, S. C., & Alves, C. C. (2015). Eliminating Schistosomes through vaccination: what are the best immune weapons? *Frontiers in Immunology, 9*, 6–95.
10. Bergquist, N. R., Leonardo, L. R., & Mitchell, G. F. (2005). Vaccine-linked chemotherapy: can schistosomiasis control benefit from an integrated approach? *Trends in Parasitology, 21*(3), 112–117.
11. Artimo, P., Jonnalagedda, M., Arnold, K., Baratin, D., Csardi, G., & de Castro, E., et al. (2012). ExPASy: SIB bioinformatics resource portal. *Nucleic Acids Research, 40*(Web Server issue), W597–603.
12. Durmuş, S., Çakır, T., Özgür, A., & Guthke, R. (2015). A review on computational systems biology of pathogen-host interactions. *Frontiers in Microbiology, 6*, 235.
13. Lopes, D. O., Oliveira, F. M., Coelho, I. E. V., Santana, K. T. O., Mendonça, F. C., Taranto, A. G., et al. (2013). Identification of a vaccine against schistosomiasis using bioinformatics and molecular modeling tools. *Infection, Genetics and Evolution, 20*, 83–95.
14. Liebenberg, J., Pretorius, A., Faber, F. E., Collins, N. E., Allsopp, B. A., & van Kleef, M. (2012). Identification of *Ehrlichia ruminantium* proteins that activate cellular immune responses using a reverse vaccinology strategy. *Veterinary Immunology and Immunopathology, 145*, 340–349.
15. Seib, K. L., Zhao, X., & Rappuoli, R. (2012). Developing vaccines in the era of genomics: a decade of reverse vaccinology. *Clinical Microbiology and Infection, 5*, 109–116.
16. Cozzi, R., Scarselli, M., & Ferlenghi, I. (2013). Structural vaccinology: a three-dimensional view for vaccine development. *Current Topics in Medicinal Chemistry, 13*, 2629–2637.
17. Agudelo, W. A., & Patarroyo, M. E. (2010). Quantum chemical analysis of MHC-peptide interactions for vaccine design. *Mini Reviews in Medicinal Chemistry, 10*, 746–758.
18. Wiens, K. E., Swaminathan, H., Copin, R., Lun, D. S., & Ernst, J. D. (2013). Equivalent T cell epitope promiscuity in ecologically diverse human pathogens. *PLoS One, 8*(8), e73124.
19. Zhu, J., & Paul, W. E. (2008). CD4 T cells: fates, functions, and faults. *Blood, 112*, 1557–1569.
20. Zhao, B., Sakharkar, K. R., Lim, C. S., Kangueane, P., & Sakharkar, M. K. (2007). MHC-peptide binding prediction for epitope based vaccine design. *International Journal of Integrative Biology, 1*, 127–140.
21. Trott, O., & Olson, A. J. (2010). Software news and update AutoDockVina: improving the speed and accuracy of docking with a new scoring function, efficient optimization, and multithreading. *Journal of Computational Chemistry, 31*, 455–461.
22. Cardoso, F. C., Pacífico, R. N., Mortara, R. A., & Oliveira, S. C. (2006). Human antibody responses of patients living in endemic areas for schistosomiasis to the tegumental protein Sm29 identified through genomic studies. *Clinical and Experimental Immunology, 144*, 382–391.
23. Ribeiro, S. P., Rosa, D. S., Fonseca, S. G., Mairena, E. C., Postól, E., & Oliveira, S. C., et al. (2010). A vaccine encoding conserved promiscuous HIV CD4 epitopes induces broad T cell responses in mice transgenic to multiple common HLA class II molecules. *PLOS One, 5*(6).
24. Lopes, D. O., Paiva, L. F., Martins, M. A., Cardoso, F. C., Rajão, M. A., Pinho, J. M., et al. (2009). Sm21.6 a novel EF-hand family protein member located on the surface of *Schistosoma mansoni* adult worm that failed to induce protection against challenge infection but reduced liver pathology. *Vaccine, 27*, 4127–4135.
25. Texier, C., Pouvelle, S., Busson, M., Hervé, M., Charron, D., Ménez, A., et al. (2000). HLA-DR restricted peptide candidates for bee venom immunotherapy. *Journal of Immunology, 164*(6), 3177–3184.

26. Case, D. A., Darden, T. A., Cheatham, T. E. I. I. I., Simmerling, C. L., Wang, J., Duke, R. E., et al. (2010). *AMBER11*. San Francisco: University of California.
27. Hawkins, G. D., Cramer, C. J., & Truhlar, D. G. (1996). Parametrized models of aqueous free energies of solvation based on pairwise descreening of solute atomic charges from a dielectric medium. *The Journal of Physical Chemistry, 100*, 19824–19839.
28. Hawkins, G. D., Cramer, C. J., & Truhlar, D. G. (1995). Pairwise solute descreening of solute charges from a dielectric medium. *Chemical Physics Letters, 246*, 122–129.
29. Duan, Y., Wu, C., Chowdhury, S., Lee, M. C., Xiong, G., Zang, W., et al. (2003). A point-charge force field for molecular mechanics simulations of proteins based on condensed-phase quantum mechanical calculation. *Journal of Computational Chemistry, 24*, 1999–2012.
30. Lee, M. C., & Duan, Y. (2004). Distinguish protein decoys by using a scoring function based a new Amber force field, short molecular dynamics simulations, and the generalized Born solvent model. *Proteins, 55*, 620–634.
31. Dennington, R., Keith, T., & Millam, J. (2009). GaussView, Version 5. Semichem Inc., Shawnee Mission KS.
32. Nakamura, S., Takahira, K., Tanabe, G., Morikawa, T., Sakano, M., Ninomiya, K., et al. (2010). Docking and SAR studies of salacinol derivatives as α-glucosidase inhibitors. *Bioorganic & Medicinal Chemistry Letters, 20*, 4420–4423.
33. Sanner, M. F. (1999). Python: a programming language for software integration and development. *Journal of Molecular Graphics & Modelling, 17*, 57–61.
34. Enviroment, D. S. M. (2012). *Accelrys software inc, release 3.1*. San Diego.
35. Pacífico, L. G., Marinho, F. A., Fonseca, C. T., Barsante, M. M., Pinho, V., Sales-Junior, P. A., et al. (2009). *Schistosoma mansoni* antigens modulate experimental allergic asthma in a murine model: a major role for $CD4^{+}$ $CD25^{+}$ $Foxp3^{+}$ T cells independent of interleukin-10. *Infection and Immunity, 77*, 98–107.
36. Boyaka, P. N., Tafaro, A., Fischer, R., Leppla, S. H., Fujihashi, K., & McGhee, J. R. (2003). Effective mucosal immunity to anthrax: neutralizing antibodies and Th cell responses following nasal immunization with protective antigen. *Journal of Immunology, 170*(11), 5636–5643.
37. Aziz, M., Yang, W. L., Matsuo, S., Sharma, A., Zhou, M., & Wang, P. (2014). Upregulation of GRAIL is associated with impaired CD4 T cell proliferation in sepsis. *Journal of Immunology, 192*(5), 2305–2314.
38. Gasteiger, J., & Marsili, M. (1980). Iterative partial equalization of orbital electronegativity—a rapid access to atomic charges. *Tetrahedron, 36*, 3219–3228.
39. Gasteiger, J., & Marsili, M. (1978). A new model for calculating atomic charges in molecules. *Tetrahedron Letters, 19*, 3181–3184.
40. Del Carpio, C. A., Hennig, T., Fickel, S., & Yoshimori, A. (2002). A combined bioinformatic approach oriented to the analysis and design of peptides with high affinity to MHC class I molecules. *Immunology and Cell Biology, 80*(3), 286–299.
41. Sette, A., & Rappuoli, R. (2010). Reverse vaccinology: developing vaccines in the era of genomics. *Immunity, 33*(4), 530–541.
42. Pinheiro, C. S., Martins, V. P., Assis, N. R. G., Figueiredo, B. C. P., Morais, S. B., Azevedo, V., et al. (2011). Computational vaccinology: an important strategy to discover new potential S. mansoni vaccine candidates. *Journal of Biomedicine & Biotechnology, 2011*, 503068.
43. Zhang, Y. L., Jia, K., Zhao, B. P., Li, Y., Yuan, C. X., Yang, J. M., et al. (2012). Identification of Th1 epitopes within molecules from the lung-stage schistosomulum of *Schistosoma japonicum* by combining prediction analysis of the transcriptome with experimental validation. *Parasitology International, 61*, 586–593.
44. Chitale, M., Hawkins, T., Park, C., & Kihara, D. (2009). ESG: extended similarity group method for automated protein function prediction. *Bioinformatics, 25*(14), 1739–4.
45. Dahl, G., & Muller, K. J. (2014). Innexin and pannexin channels and their signaling. *FEBS Letters, 588*(8), 1396–1402.
46. Bissantz, C., Kuhn, B., & Stahl, M. (2010). A medicinal chemist's guide to molecular interactions. *Journal of Medicinal Chemistry Perspective, 53*(14), 5061–5084.
47. Zhu, Y., Rudensky, A. Y., Corper, A. L., Teyton, L., & Wilson, I. A. (2003). Crystal structure of MHC class II I-Ab in complex with a human CLIP peptide: prediction of an I-Ab peptide-binding motif. *Journal of Molecular Biology, 326*(4), 1157–1174.
48. Gilson, M. K., & Honig, B. H. (1987). Calculation of electrostatic potentials in an enzyme active-site. *Nature, 330*, 84–86.
49. Weiner, P. K., Langridge, R., Blaney, J. M., Schaefer, R., & Kollman, P. A. (1982). Electrostatic potential molecular-surfaces. *Proceedings of the National Academy of Sciences of the United States of America, 79*, 3754–3758.

50. Dewar, M. J. S., Zoebisch, E. G., Healy, E. F., & Stewart, J. J. P. (1985). The development and use of quantum mechanical molecular models.76. Am1—a new general purpose quantum mechanical molecular-model. *Journal of the American Chemical Society, 107*, 3902–3909.
51. Halgren, T. A. (1996). Merck molecular force field 3. Molecular geometries and vibrational frequencies for MMFF94. *Journal of Computational Chemistry, 17*, 553–586.
52. Tsai, K. C., Wang, S. H., Hsiao, N. W., Li, M., & Wang, B. (2008). The effect of different electrostatic potentials on docking accuracy: a case study using DOCK5.4. *Bioorganic & Medicinal Chemistry Letters, 18*, 3509–3512.
53. Engelhard, V. H. (1994). Structure of peptides associated with class I and class II MHC molecules. *Annual Review of Immunology, 12*, 181–207.
54. Zhao, B. P., Chena, L., Zhanga, Y. L., Yanga, J. M., Jiaa, K., Sui, C. Y., et al. (2012). In silico prediction of binding of promiscuous peptides to multiple MHC class-II molecules identifies the Th1 cell epitopes from secreted and transmembrane proteins of *Schistosoma japonicum* in BALB/c mice. *Microbes and Infection, 13*(7), 709–719.
55. Cook, P. C., Aynsley, S. A., Turner, J. D., Jenkins, G. R., Van Rooijen, N., Leeto, M., et al. (2011). Multiple helminth infection of the skin causes lymphocyte hypo-responsiveness mediated by Th2 conditioning of dermal myeloid cells. *PLoS Pathogens, 7*, 1–14.